analytical chemistry

pubs.acs.org/ac Article

Dual-Luciferase-Based Fast and Sensitive Detection of Malaria Hypnozoites for the Discovery of Antirelapse Compounds

Annemarie M. Voorberg-van der Wel, Anne-Marie Zeeman, Ivonne G. Nieuwenhuis, Nicole M. van der Werff, Els J. Klooster, Onny Klop, Lars C. Vermaat, and Clemens H. M. Kocken*

Cite This: *Anal. Chem.* 2020, 92, 6667−6675

Read Online

ACCESS | Metrics & More | Article Recommendations | Supporting Information

ABSTRACT: Efforts to eradicate *Plasmodium vivax* malaria are hampered by the presence of hypnozoites, persisting stages in the liver that can reactivate after prolonged periods of time enabling further transmission and causing renewed disease. Large-scale drug screening is needed to identify compounds with antihypnozoite activity, but current platforms rely on time-consuming high-content fluorescence imaging as read-out, limiting assay throughput. We here report an ultrafast and sensitive dual-luciferase-based method to differentiate hypnozoites from liver stage schizonts using a transgenic *P. cynomolgi* parasite line that contains Nanoluc driven by the constitutive *hsp70* promoter, as well as firefly luciferase driven by the schizont-specific *lisp2* promoter. The transgenic parasite line showed similar fitness and drug sensitivity profiles of selected compounds to wild type. We demonstrate robust bioluminescence-based detection of hypnozoites in 96-well and 384-well plate formats, setting the stage for implementation in large scale drug screens.

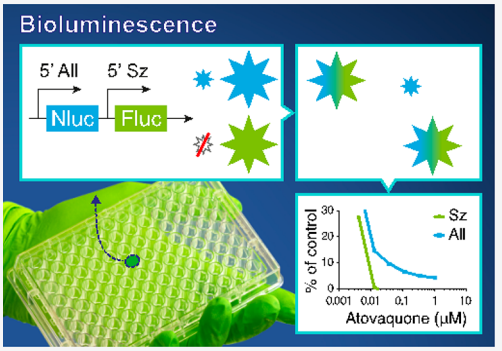

Almost half of the world's population is at risk of malaria, with *Plasmodium vivax* being a major causative agent of malaria in many countries outside of sub-Saharan Africa.[1] Symptoms of malaria caused by *P. vivax* can be severe and may even lead to mortality.[2,3] Recognizing the enormous morbidity and mortality burden due to malaria, in 2015 the World Health Assembly adopted a Global Technical Strategy for malaria 2016−2030[4] which aims to reduce the global malaria disease burden by 90% and to eliminate malaria in at least 35 countries by 2030. The complex biology of *P. vivax*, however, presents a major obstacle in the elimination of malaria. In contrast to the other major malaria parasite *P. falciparum, P. vivax* can develop into hypnozoites, persisting forms in the liver that can reactivate after prolonged periods of time, to not only give rise to new transmissible stages but also to cause new episodes of malaria.[5,6] To date, hypnozoites can only be eliminated by 8-aminoquinolines, such as primaquine and tafenoquine.[7,8] However, these drugs can cause severe side-effects in people with glucose-6-phosphate dehydrogenase (G6PD) deficiency.[9] This limited arsenal of drugs with antihypnozoite activity, combined with their restrictions for usage, spurs new research toward finding formulations that can effectively eliminate these parasite stages.

In the absence of an in vitro blood stage culture, access to P. vivax parasites is dependent on patient material, complicating *P. vivax* research. Notwithstanding these challenges, much progress has been made over the past few years, resulting in different in vitro liver stage platforms in which compounds can be tested for activity against hypnozoites.[10−13] The read-out of these assays relies on high-content fluorescence imaging to distinguish small (hypnozoites) from large (developing) forms, which limits the throughput of the assay because of the time-consuming imaging and analysis. For example, in our current workflow that uses high-content imaging and analysis, it takes about a week to obtain the raw data from ten 96-well plates after harvesting. For higher-throughput assays, bioluminescent read-outs have recently gained popularity because of the speed, robustness, and high dynamic ranges provided by this type of measurements.[14] High-throughput luciferase-based assays using transgenic *P. berghei* rodent malaria parasites have already been used to screen thousands of compounds for activity against liver stages.[15,16] However, rodent malaria liver stages only require 2−3 days for full development, whereas primate malarias require 7−10 days. Moreover, rodent malaria parasites do not form hypnozoites.

Hypnozoites are only present in several primate malarias, including the close simian relative of *P. vivax, P. cynomolgi. P. cynomolgi* is considered to be the gold standard for hypnozoite research[17] and is more amenable to experimentation than *P. vivax*, which has resulted in an extended toolbox that includes

Received: February 7, 2020
Accepted: April 8, 2020
Published: April 8, 2020

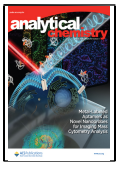

https://dx.doi.org/10.1021/acs.analchem.0c00547
Anal. Chem. 2020, 92, 6667−6675

robust transfection technology.[18−20] This has allowed comprehensive transcriptomic analysis of hypnozoites and liver schizonts revealing significantly reduced transcription levels in hypnozoites.[21,22] Unfortunately, a marker gene specific for hypnozoites was not found, rendering it impossible to develop a reporter parasite based on a hypnozoite-specific promoter.

To overcome these issues, we here report the development and application of a dual-bioluminescent reporter parasite to detect hypnozoite- as well as schizont-derived signals in a reporter assay. Using this new transgenic *P. cynomolgi* line in which both the bright luciferase *nanoluc* (Nluc),[23,24] driven by the constitutive *hsp70* promoter, and *firefly luciferase* (Fluc), driven by the recently described schizont-specific *liver stage specific protein-2* (*lisp2*)[25] promoter, are expressed, drug activity against schizonts as well as hypnozoites can be monitored at high speed and robustness in a format that is scalable to high-throughput screening.

EXPERIMENTAL SECTION

Plasmid Construction. Previously we have described a *P. cynomolgi* transgenic line that besides fluorescent reporter genes also includes *nluc* under control of *lisp2* regions[26] (here called 'Sz_Nluc'). To create the 'All_Nluc' line, a centromere construct pCyCEN_Lisp2Fluc_hsp70Nluc was developed which is essentially the same as the pCyCEN_Lisp2mCherry_hsp70_GFP plasmid constructed to generate 'Sz_Nluc'.[26] The fluorescent markers GFP and mCherry were replaced with Nluc (linked to Hdhfr with t2a) and Fluc, respectively. The plasmid was made with Plasmid # 1 and # 2[26] and a previously described centromere plasmid.[20] The cloning scheme and sequences of new building blocks are described in the Supporting Information file (Figure S1). A synthetic version (*luc2*) of the *fluc* gene (as in NCBI QBQ18419.1) flanked by *Bgl*II/ *Eco* RV sites was synthesized in a source plasmid (Genscript), *Bgl*II/ *Eco* RV digested and cloned into the *Bgl*II/ *Eco* RV sites of "Plasmid #2"[26] to generate "Plasmid X". The *hdhfr* selection cassette from 'Plasmid #3'[26] was replaced by a *Spe* I/ *Cla* I digested fragment from a source plasmid containing *hdhfr* linked with *t2a* to *nluc* (synthesized by Genscript) to generate "Plasmid Y". The *fluc* expression cassette of "Plasmid X" was *Bam*HI/ *Kpn*I cloned into "Plasmid Y" to generate 'Plasmid X_Y'. This plasmid was *Not* I digested and ligated to *Not* I linearized plasmid pCR-BluntII-TOPO containing a *P. cynomolgi* centromere;[20] Genbank accession number JQ809338) to generate the final construct pCyCEN_Lisp2Fluc_hsp70Nluc.

Nonhuman Primates—Ethics Statement. Nonhuman primates were used because no other models (in vitro or in vivo) were suitable for the aims of this project. Prior to the start of the experiments, the research protocol (agreement number #007C under CCD license number AVD5020020172664) and subprotocol (BPRC Dier Experimenten Commissie, DEC; agreement number #708) were approved by the central committee for animal experiments and by the local independent ethical committee and the local 'Instantie voor Dierenwelzijn' (IvD) constituted conform Dutch law, respectively. All experiments were performed according to Dutch and European laws. The Council of the Association for Assessment and Accreditation of Laboratory Animal Care (AAALAC International) has awarded BPRC full accreditation. Thus, BPRC is fully compliant with the international demands on animal studies and welfare as set forth by the European Council Directive 2010/63/EU, and Convention ETS 123, including the revised Appendix A as well as the 'Standard for humane care and use of Laboratory Animals by Foreign institutions' identification number A5539-01, provided by the Department of Health and Human Services of the United States of America's National Institutes of Health (NIH) and Dutch implementing legislation. The health of the animals is checked at least once a year. Prior to experimentation an additional health check is carried out, including a physical examination and performing hematological, clinical-chemistry, serology, and bacteriological and parasitological analyses. Only healthy animals were included in the experiments. The rhesus monkeys used in this study (*Macaca mulatta*, either gender, 5−7 years, Indian origin) were captive-bred and socially housed. Animal housing was according to international guidelines for nonhuman primate care and use. Besides their standard feeding regime and drinking water ad libitum via an automatic watering system, the animals followed an environmental enrichment program. Next to permanent and rotating nonfood enrichment, the macaques were offered an item of food-enrichment on a daily basis. All animals were monitored daily for health and discomfort. Monkeys were trained to voluntarily present for thigh pricks and were rewarded afterward. Ketamine sedation was applied for all intravenous injections and large blood, and all efforts were made to minimize suffering. Liver cells were derived from in-house frozen batches of hepatocytes or from freshly collected liver lobes from monkeys that were euthanized in the course of unrelated studies (ethically approved by the BPRC DEC) or euthanized for medical reasons, as assessed by a veterinarian. Therefore, none of the animals from which liver lobes were derived were specifically used for this work, according to the 3Rrule thereby reducing the numbers of animals used. Euthanasia was performed under ketamine sedation (10 mg/kg) and was induced by intracardiac injection of euthasol 20%, containing pentobarbital.

Transfection of *P. cynomolgi*. *P. cynomolgi* M strain blood stage parasites originally provided by Dr. Bill Collins from the Center for Disease Control, Atlanta, USA[27] were thawed and resuspended in PBS for i.v. injection (10^6 parasites in 1 mL PBS) into a donor monkey. Parasitemia was monitored by thigh prick and at peak parasitemia (±1% trophozoites) heparin blood was collected and the monkey was cured from malaria parasites by chloroquine treatment (i.m., 7.5 mg/kg, on 3 consecutive days). Parasites were enriched using a 55% Nycodenz/PBS cushion and centrifuged (25 min, 300 g, RT, low brake). The interface, containing ±30% trophozoites was collected, washed, and cultured overnight as described previously.[26] The following day, parasites (schizonts) were harvested and transfected using two methods as described before[26] to increase chances of obtaining successfully transfected parasites. For one method a Nucleofector device (Lonza, program U-033) was used to transfect 2×10^7 parasites in 100 μL Human T-Cell Nucleofector solution (Lonza) with 10 μg of plasmid DNA. The other method used electroporation (settings 25 μF, 2500 V and 200 Ω) using a 4 mm electroporation cuvette (Bio-Rad) to transfect $\pm 3 \times 10^8$ parasites resuspended in Cytomix (120 mM KCl, 0.15 mM $CaCl_2$, 2 mM EGTA, 5 mM $MgCl_2$, 10 mM K_2HPO_4, 10 mM KH_2PO_4, 25 mM Hepes, pH 7.6) with 45 μg of plasmid DNA. The electroporated samples were combined in 0.5 mL PBS and injected into a recipient monkey. Starting 1 day post infection, the recipient monkey was treated with 4 dosages of

https://dx.doi.org/10.1021/acs.analchem.0c00547
Anal. Chem. 2020, 92, 6667−6675

pyrimethamine (1 mg/kg, orally in a piece of fruit every other day), to eliminate wild type parasites that had not been transfected. The first drug resistant parasites emerged at day 11 post transfection. Around peak parasitemia blood was obtained for stocks and mosquito feeding. Immediately thereafter, the donor monkey was cured with chloroquine (i.m., 7.5 mg/kg, on 3 consecutive days).

Mosquito Feeding. Recipient monkeys were i.v. injected with 1×10^6 transgenic *P. cynomolgi* M strain blood stage parasites from a cryopreserved stock. The monkeys received 3 dosages of pyrimethamine (1 mg/kg, orally in a piece of fruit every other day) to eliminate possible wild type contaminant parasites. The course of infection was monitored by Giemsa stained thin blood films obtained from thigh pricks. Heparin blood (5−9 mL) for mosquito feeding was collected around peak parasitemia on two (usually consecutive) days, generally around day 11−13 post infection. Immediately thereafter, monkeys were cured with chloroquine (i.m., 7.5 mg/kg, on 3 consecutive days). *Anopheles stephensi* mosquitoes Sind-Kasur strain Nijmegen[28] (aged 2−5 days) were obtained from Nijmegen UMC, The Netherlands and fed on the infected blood using a water-jacketed glass feeder system kept at 37 °C. Mosquitoes were housed for approximately 3 weeks in climate chambers at 25 °C and 80% humidity and were fed daily via cotton soaked in 5% D-glucose solution. One week after infection oocysts were counted and mosquitoes were given an additional uninfected blood meal to promote sporozoite invasion of the salivary glands.

Primary Rhesus Hepatocyte Cultures. Primary hepatocyte cultures were initiated either from freshly isolated *Macaca mulatta* hepatocytes through collagenase perfusion[29] or from in-house cryopreserved stocks. Hepatocytes were seeded into collagen coated 96-well CellCarrier Ultra plates (PerkinElmer) at a density of $\pm 65 \times 10^3$ cells/well or into 384-well collagen coated ViewPlate plates at a density of $\pm 25 \times 10^3$ cells/well in William's B medium (William's E with glutamax containing 10% human serum (A+), 1% MEM nonessential amino acids, 2% penicillin/streptomycin, 1% insulin/transferrin/selenium, 1% sodium pyruvate, 50 μM β-mercapto-ethanol, and 0.05 μM hydrocortisone). Following cell attachment, cells were maintained in William's B medium containing 2% dimethyl sulfoxide (DMSO) to prevent hepatocyte dedifferentiation. Prior to adding sporozoites, cells were washed twice in William's B medium. Liver stage cultures were maintained in William's B medium in a humidified incubator at 37 °C and at 5% CO_2.

***P. cynomolgi* Sporozoite Isolation and Liver Stage Culture.** Two weeks post mosquito feeding salivary gland sporozoites were isolated and used for hepatocyte inoculation. Salivary glands were collected on ice in Leibovitz's medium containing 3% FCS and 2% Pen/Strep. Salivary glands were disrupted using a Potter-Elvehjem homogenizer, and debris was removed by a slow spin in a microfuge (3 min, 60 g, RT), before counting the sporozoites in a Bürker-Türk counting chamber. Primary rhesus hepatocytes seeded 2−3 days earlier were inoculated with 5×10^4 sporozoites per well (96-well plates) or 2×10^4 sporozoites per well (384-well plates) in William's B medium. Plates were spun for 5 min at 233g (RT, low brake), incubated for 2−3 h to allow for sporozoite invasion (at 37 °C and at 5% CO_2), and after washing with William's B medium incubation was continued with regular medium refreshments (with or without drugs). Drugs were obtained from the Novartis Institute for Tropical Disease (NITD; PI4K inhibitor compound **17**[30] and KAF156) and Medicines for Malaria Venture (MMV; atovaquone). At day 6 post sporozoite inoculation cultures were harvested for bioluminescence measurement or for fixation with 4% paraformaldehyde (PFA) for 30 min at room temperature.

High Content Imaging (HCI). For high content imaging using an Operetta (PerkinElmer), fixed cultures were incubated overnight at 4 °C with rabbit anti-*P. cynomolgi* HSP70 primary antibody diluted 1:10,000 in antibody dilution buffer (0.3% Triton-X100, 1% BSA in PBS). Samples were washed with PBS and incubated for 2 h at room temperature with Alexa 647-conjugated goat-antirabbit IgG (Thermo Fisher Scientific, 1:1000) and 2 μM 4′,6-diamidino-2-phenylindole, dilactate (DAPI, Thermo Fisher Scientific) in antibody dilution buffer. Samples were washed again in PBS, and images were captured on the Operetta. Parasites were counted by using a custom script in the Operetta Harmony/Columbus 2.8.2 (PerkinElmer) software, essentially as described before.[11] Data were analyzed using Prism 8.0 (GraphPad Software).

Bioluminescence Measurements. Bioluminescence was measured using the Nano-Glo Dual-luciferase Reporter (NanoDLR) assay system (Promega), according to the manufacturer's instructions. Briefly, cultures were equilibrated at room temperature. Culture medium was replaced with 50 μL of PBS/well (in 96-well plates). 50 μL of OneGlowEx was added and mixed on an orbital shaker ($\pm$400 rpm) for 3−5 min at room temperature. Fluc activity was then measured by a Victor Multilabel Plate reader (PerkinElmer) at 1 s/well. Subsequently, 50 μL of NanoDLR Stop & Glo Reagent (diluted 1:100) was added per well, mixed for 10 min on an orbital shaker ($\pm$600 rpm) before measuring Nluc activity by the Victor Multilabel Plate reader (PerkinElmer) at 1 s/well. For bioluminescence measurements in 384-well plates reagent amounts were halved. Data were analyzed using Prism 8.0 (GraphPad Software).

RESULTS AND DISCUSSION

Development and Fitness of *P. cynomolgi* Expressing Nanoluc (Nluc) and Firefly Luciferase (Fluc). A hypnozoite-specific promoter to drive expression of a bioluminescent reporter would greatly facilitate the development of a hypnozoite-specific reporter line. Unfortunately, a hypnozoite-specific marker gene has not been identified in the *P. cynomolgi* hypnozoite transcriptome.[21,22] To still enable detection of hypnozoite signals, we have developed a dual reporter parasite line (called 'All_Nluc') in which one reporter is constitutively expressed by all liver stage parasites, whereas the other reporter is only expressed in liver stage schizonts. Upon drug treatment with a compound that eliminates the schizonts, as measured by a complete loss of the schizont specific reporter signal, the remaining signal would be derived from the constitutively expressed reporter in the hypnozoites. Recently, the very bright bioluminescent reporter Nanoluc was shown to enable ultrasensitive detection of different parasite developmental stages of *P. berghei*[31] and *P. falciparum*.[32] We therefore hypothesized that the signals derived from the Nluc reporter might be bright enough to even detect a silent parasitic stage such as a hypnozoite. To further maximize signal output, a plasmid was designed with Nluc under control of the strong constitutive *P. cynomolgi hsp70* promoter.[26] Separated by a self-cleaving peptide T2A to reduce the construct size,[33] the selectable marker *human dihydrofolate reductase* (*dhfr*) was included in this *hsp70*-driven expression cassette. To detect

https://dx.doi.org/10.1021/acs.analchem.0c00547
Anal. Chem. 2020, 92, 6667−6675

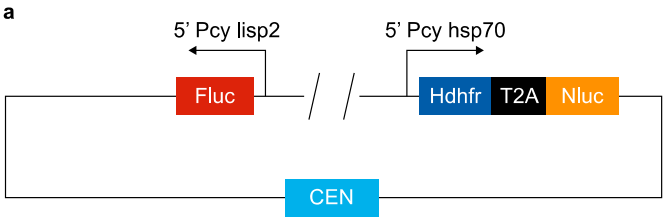

c

	Feed 1		Feed 2	
	Average # oocysts per inf. midgut	# Infected	Average # oocysts per inf. midgut	# Infected
WT	9	10/10	185	10/10
All_Nluc' line	45	10/10	>200	10/10

	Feed 2	
	Spz/mosq	# mosq
WT	67,5 x 10e3	252
All_Nluc' line	94,5 x 10e3	146

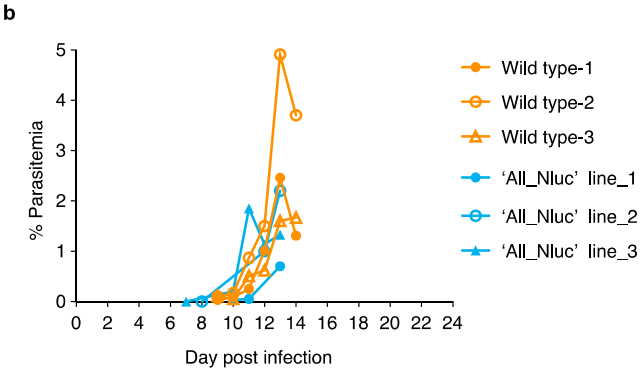

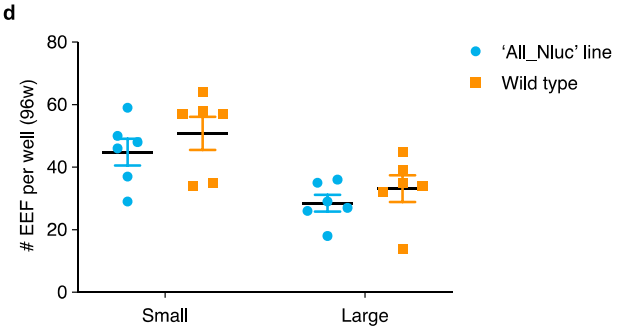

Figure 1. Construction and fitness of the *P. cynomolgi* 'All_Nluc' reporter line. (a) Schematic representation of the most important elements of the construct used for transfection. (b) Blood stage parasitemia of the 'All_Nluc' line (blue lines) compared to the development of wild type *P. cynomolgi* (WT; orange lines) after infection with blood stage parasites from a cryopreserved stock. (c) Oocyst counts (day 7 post feeding) of *P. cynomolgi* wild type (WT) and reporter line 'All_Nluc' infected *A. stephensi* mosquitoes fed on 2 consecutive days post blood stage infection. The lower table shows the number of salivary gland sporozoites obtained after mosquito dissection (at day 14 post feeding). (d) Number of small and large exoerythrocytic forms (EEF) per well (with mean ± s.e.m.) in 6 wells of a 96-well plate at day 6 post sporozoite infection with wild type *P. cynomolgi* sporozoites (orange) or 'All_Nluc' sporozoites (blue).

schizont-specific bioluminescence, an additional expression cassette was included with Fluc under control of 5′ and 3′ UTRs of *P. cynomolgi lisp2*, a gene that is specifically expressed in *P. cynomolgi* liver schizonts and not in hypnozoites.[25] Schizont-specific expression of a fluorescent reporter under control of these *lisp2* UTRs has previously been shown.[26] A *P. cynomolgi* centromere was incorporated to stably maintain the construct throughout the life cycle[20] (Figure 1a). For transfection, *P. cynomolgi* M-strain blood stage trophozoites were isolated from a donor monkey, and following a parasite purification and a short-term cultivation step to obtain mature blood stage schizonts,[20] parasites were electroporated and injected into a recipient monkey. Pyrimethamine-resistant parasites emerged and stocks were made. Blood stage development of the transgenic parasites was similar to wild-type parasites (Figure 1b). A side-by-side comparison of transmission characteristics showed similar numbers of oocysts for transgenic and wild type parasites (Figure 1c). The number of salivary gland sporozoites per mosquito was also comparable for the wild type (67.5×10^3) and the 'All_Nluc' line (94.5×10^3) (Figure 1c). Similar numbers were obtained in further transmissions with the 'All_Nluc' line, which showed that *A. stephensi* salivary glands contained on average 80.5×10^3 'All_Nluc' sporozoites $\pm 29.5 \times 10^3$ per mosquito (4 independent infections; derived from 172 ± 51 dissected mosquitoes per infection). Upon infection of primary hepatocytes, exoerythrocytic (EEF) numbers were similar for transgenic and wild type parasites (small forms: 45 ± 10 ('All_Nluc') versus 51 ± 13 (wild type); large forms: 29 ± 7 ('All_Nluc') versus 33 ± 10 (wild type)) (Figure 1d). In both lines this results in 61% percent small forms. Taken together, this indicates that the parasite fitness had not been affected by the introduction of the construct.

Dual Reporter Line That Shows Differential Timing of Bioluminescent Protein Expression in Liver Stages. In *P. cynomolgi* liver stages, the Lisp2 protein is expressed in multinucleate parasites, starting at the onset of liver stage schizogony, 3 days post sporozoite infection.[25] A similar stage-specific expression was also observed in a *P. cynomolgi* fluorescent reporter line that showed schizont-specific expression of mCherry controlled by *lisp2* flanking regions.[26] This reporter line, which shows a fitness comparable to wild-type parasites,[26] additionally contains the bioluminescent reporter Nluc linked by T2A[33] with mCherry under control of *lisp2*.[26] We here use this single bioluminescent 'Sz_Nluc' line as a reference for the dual 'All_Nluc' line which contains the Fluc bioluminescent reporter driven by *lisp2* (Figure 1a) to control for possible confounding data arising from a previously described 150-fold lower brightness of Fluc compared to Nluc.[23,31] To characterize the temporal kinetics of the bioluminescent signals of the dual reporter throughout liver stage development, a time course experiment was performed. Following sporozoite infection of primary hepatocytes, triplicate wells of 96-well plates containing dual reporter line 'All_Nluc' parasites, single reporter line 'Sz_Nluc' parasites with Nluc controlled by *lisp2*,[26] or noninfected hepatocytes

https://dx.doi.org/10.1021/acs.analchem.0c00547
Anal. Chem. 2020, 92, 6667−6675

were harvested at different time points. Bioluminescence was measured using a Promega Nanoglo Dual-luciferase Reporter (NanoDLR, Promega) system which first detects Fluc, followed by complete quenching and subsequent measurement of Nluc. Background levels of uninfected hepatocytes measured in two experiments showed negligible counts for both Fluc and Nluc (average RLU < 36 ± 93). Measurements of Nluc (in the single reporter 'Sz_Nluc' line) and Fluc (in the dual reporter 'All_Nluc' line) signals controlled by the *lisp2* promoter show some background bioluminescence at days 1 and 2, whereas from day 3 onward expression levels steeply rise until the end of schizogony (Figure 2). Notwithstanding the much brighter expression of *lisp2* driven Nluc in the 'Sz_Nluc' line compared to the *lisp2* driven Fluc in the 'All_Nluc' dual reporter line, in line with the previously described 150-fold higher brightness of Nluc compared to Fluc,[23,31] the pronounced increase in signal over time was similar in both lines.

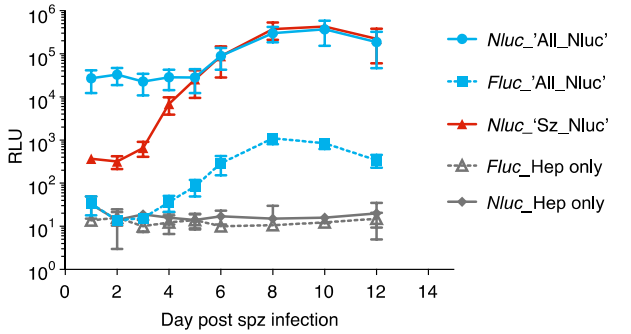

Figure 2. Total Firefly luciferase (Fluc) and Nanoluc (Nluc) bioluminescence signals measured in the *P. cynomolgi* dual reporter ('All_Nluc') reporter line (blue) and the single reporter ('Sz_Nluc') control line (red) at different time points post sporozoite infection of primary rhesus hepatocytes. Results are expressed as average Relative Light Units (RLU) ± s.d. of three independent infections in 96-well plates (triplicate wells each). For reference, background Fluc and Nluc counts are depicted of uninfected hepatocytes from one experiment (gray lines, triplicate wells ± s.d.).

In contrast, Nanoluc driven by the *hsp70* promoter in the All_Nluc line already yielded high RLU values that remained relatively constant from day 1 after sporozoite infection onward (Figure 2), reflecting the constitutive expression pattern of *hsp70*. Though less pronounced than in the *lisp2*-driven reporters, there was a signal increase observed during schizogony (most notably starting at day 6), most likely as a result of the enormous increases in parasite biomass that occurs during liver stage development.

Drug Sensitivity of Transgenic Reporter Lines Is Similar to Wild-Type Parasites. Before embarking on drug sensitivity assays relying on bioluminescence, we first compared the sensitivity of wild-type and transgenic schizonts and hypnozoites to a selected set of compounds using traditional high-content imaging as the read-out system.

As expected, IC_{50} curves (Figure 3) and IC_{50} values (Table S1) obtained from a drug assay in which primary rhesus hepatocytes were inoculated side by side with transgenic and wild-type *P. cynomolgi* sporozoites were highly similar, indicating that drug sensitivity profiles had not changed as a result of the presence of the centromeric constructs. As shown before,[11] liver stage schizonts are markedly more sensitive to atovaquone and KAF156 treatment (day 0−6) than hypnozoites. In contrast, treatment (day 0−6) with the PI4K inhibitor ("compound 17"[30]) affects both stages.

It should be noted that the transgenic *P. cynomolgi* lines do contain a selectable marker that confers antifolate resistance, so compounds with antifolate activity cannot be tested in this system. For testing compounds with antihypnozoite activity, this most likely is not a problem. Antifolates are inhibiting DNA synthesis, which does not occur in hypnozoites, and pyrimethamine, an antifolate compound, has not shown any activity against hypnozoites.[11]

Bioluminescence-Based Drug Sensitivity Curves of Liver Stage Parasites. Next, it was determined whether drug sensitivity of total liver stage parasites and schizonts of the 'All_Nluc' line could be measured by bioluminescence with the dual reporter system. Upon day 0−6 treatment with the PI4 kinase inhibitor similar IC50 curves for total liver stage parasites counted by high-content imaging (HCI) and by bioluminescence (as measured by Nluc) were obtained (Figure 4a). The drug sensitivity of schizonts could be separately determined by measuring Fluc signals (Figure 4b). Bioluminescence measurements indicated a trend toward slightly lower IC50 values as has been described earlier for the rodent malaria *P. berghei* reporter lines.[16]

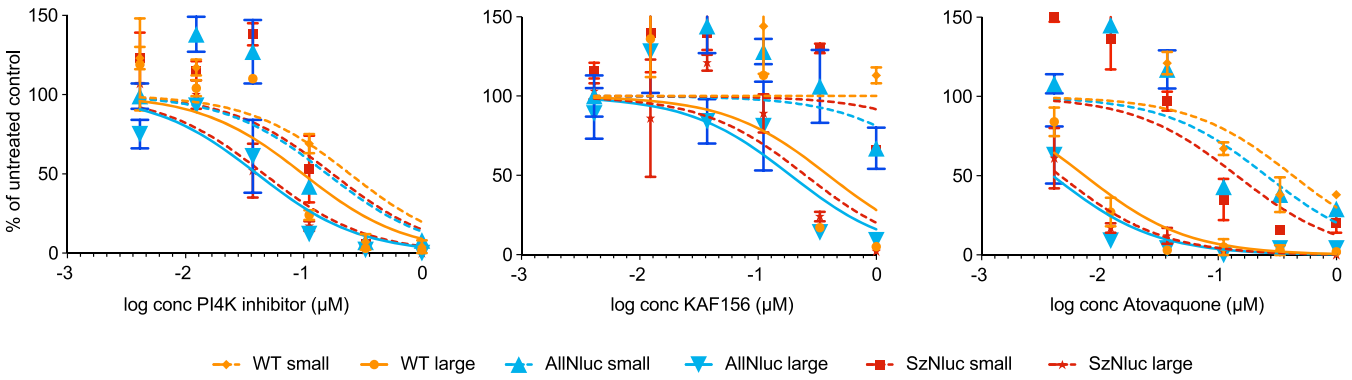

Figure 3. Image-based drug sensitivity curves of fixed and stained *P. cynomolgi* reporter lines and wild-type parasites treated from day 0−6 with different concentrations of a PI4K inhibitor, KAF156 or Atovaquone. Small and large parasites of wild type ("WT", orange), dual reporter line ('All_Nluc', blue), and the single reporter control line ('Sz_Nluc', red) were counted using Harmony software (PerkinElmer). Curve fitting was performed using the least-squares nonlinear regression method (GraphPad Prism) for small and large parasites. Results are expressed as mean ± s.d. from duplicate wells from one representative experiment. Assays were performed at least twice.

https://dx.doi.org/10.1021/acs.analchem.0c00547
Anal. Chem. 2020, 92, 6667−6675

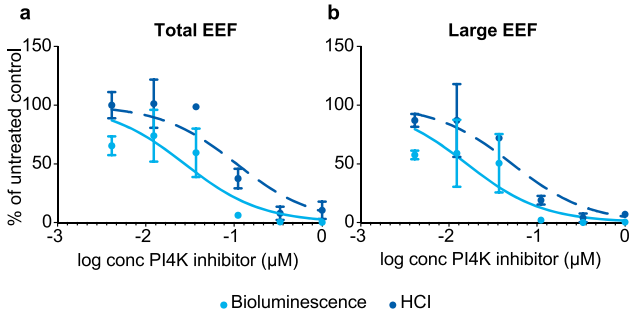

Figure 4. Bioluminescence- and image-based drug sensitivity curves of the *P. cynomolgi* 'All_Nluc' line treated from day 0−6 with PI4K inhibitor. (a) Total EEF numbers assessed by HCI and by measuring Nluc signals and (b) numbers of liver stage schizonts ("Large EEF") assessed by HCI and by measuring Fluc signals in drug treated wells relative to untreated controls. Results are expressed as mean ± s.d. from duplicate wells from one representative experiment. Assays were performed at least twice.

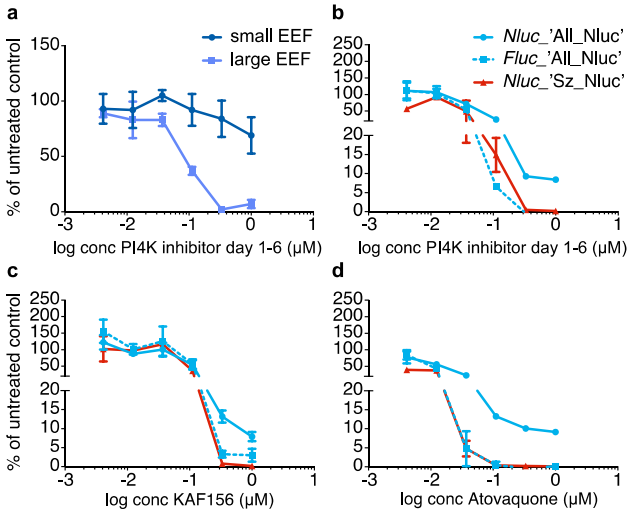

Figure 5. Bioluminescence-based detection of *P. cynomolgi* hypnozoites following differential drug treatment. (a) Drug sensitivity curves of *P. cynomolgi* 'All_Nluc' treated day 1−6 with PI4kinase inhibitor. Small EEF (hypnozoites) and large EEF (schizonts) were counted by HCI and counts were compared to untreated wells. (b, c, d) Bioluminescence-based drug sensitivity curves for day 1−6 PI4kinase inhibitor (b), day 0−6 KAF156 (c), and atovaquone (d) treated liver stage parasites. Nluc signals (solid lines) are expressed relative to untreated control wells for the 'All_Nluc' (blue) and the 'Sz_Nluc' line (red). Fluc signals (dotted lines) are expressed relative to untreated control wells ('All_Nluc' line, blue). Results are expressed as mean ± s.d. from duplicate wells from one representative experiment. Assays were performed at least twice.

Given that it was possible to separately measure schizonts (Fluc) and total parasites (Nluc), we next investigated whether it is feasible to detect Nluc signals derived from hypnozoites only, by applying drug treatments that differentially target schizonts.

Bioluminescence-Based Detection of Hypnozoites. PI4kinase inhibitors are known to act early in the development of liver stage parasites,[34,35] and in vitro drug treatment starting at 1 day post inoculation or later has shown differential killing activity of schizonts, whereas hypnozoites are far less affected.[25,32] When measured by HCI, we indeed observed that upon day 1−6 treatment with the PI4K inhibitor, schizonts were killed, whereas hypnozoites largely survived this treatment (Figure 5a).

Similarly, the bioluminescent read-out of the d1-6 PI4K inhibitor-treated single bioluminescent "Sz-Nluc" line (Figure 5b, red line) showed that schizont-specific *lisp2* driven Nluc signals dropped to zero, indicating that all schizonts were killed. Similarly, the Fluc levels of the "All-Nluc" line (also controlled by *lisp2*) also dropped to background levels after day 1−6 treatment with the PI4K inhibitor. In contrast, the Nluc signals from the "All-Nluc" line, controlled by the constitutive *hsp70* regions, did not decrease to background levels, but instead ±10% of the Nluc signal from the untreated control remained present at high PI4K inhibitor concentrations (Figure 5b). As the only parasites not affected by these PI4K inhibitor concentrations are the hypnozoites (Figure 5a), these Nluc signals derive from hypnozoites only.

Interestingly, hypnozoites, that constitute ±60% of the liver stage parasite population (Figure 1d), account for only 10% of the total Nluc signal, likely due to the reported low gene expression levels at day 6.[21] The differential killing activity of the d1−6 versus d0−6 PI4K inhibitor treatment as measured both by HCI and by bioluminescence is further highlighted in Table S2 and Figure S2. These data show that after d0-6 treatment, which kills all parasites as measured by HCI, both Fluc and Nluc signals drop to background levels. In marked contrast, after d1-6 treatment, only hypnozoites remain present, as measured by HCI. This results in background Fluc levels but clear RLU values for Nluc.

This was further demonstrated by measuring the signals of cultures treated with atovaquone and KAF156. These compounds are known to kill developing liver stages and to not affect hypnozoites,[11] as was also observed for the reporter lines by imaging of fixed parasites after treatment (Figure 3). Bioluminescence measurements of treated cultures indeed showed a decrease in schizont-specific Fluc signal, which at higher compound concentrations, reaches negligible levels compared to the untreated control (Figure 5c and d, dotted blue lines). This indicates effective killing of schizonts. While the Nluc signal in the "All-Nluc" line also showed a decrease, the signals remained significantly (to ±5−10% of the untreated control) above background levels. This reflects the Nluc levels expressed by the hypnozoite population (Figure 5c and d, solid blue lines) that remains present at these concentrations, as determined by HCI (Figure 3). This observation is strengthened by the finding that Nluc driven by the schizont-specific *lisp2* promoter in the reference 'Sz_Nluc' line shows negligible signals compared to the untreated controls following treatment with atovaquone or KAF156, again indicating effective killing of liver stage schizonts (Figure 5c and d, red lines).

Taken together, these data demonstrate that hypnozoites can be detected based on bioluminescent Nluc signals in the *P. cynomolgi* 'All_Nluc' line, after killing of all developing parasites. A high throughput screening of hypnozoiticidals can thus be envisaged either by screening in combination with a schizont-killing drug, or the schizont-killing drug treatment could be performed prior to the drug screening. The latter would avoid potential interference of the effect of the schizont killing compound with the compounds to be tested. The speed of the dual-reporter bioluminescence assay is unprecedented, as, depending on the system used, signal read-out per well takes only 0.1−1 s. We estimate that the time from harvesting to raw data for ten 96-well plates would require less than an

https://dx.doi.org/10.1021/acs.analchem.0c00547
Anal. Chem. 2020, 92, 6667−6675

hour, which is superior to the estimated week that is required by currently available methods for hypnozoite drug screening.

Bioluminescence-Based Detection of Hypnozoites in 384-well Plate Format. The work described above was all performed in 96-well plates. However, for higher throughput assays, to reduce the cost per well, miniaturization is warranted. Therefore, we tested whether it would be feasible to detect reporter parasites by bioluminescence in a 384-well plate format. Bioluminescence read outs of hepatocytes inoculated with serial sporozoite dilutions of the 'All_Nluc' line in 384-well plates showed signal intensities that were proportional to the number of parasites present in the well (as assessed by HCI) (Figure 6). Even at the lowest (5000)

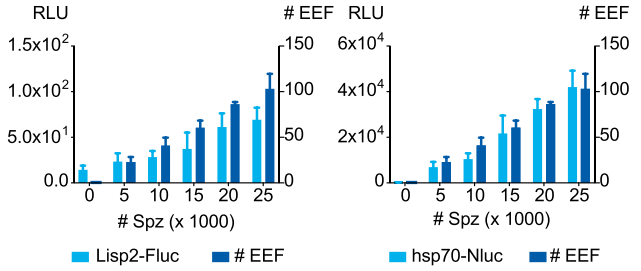

Figure 6. Bioluminescence and HCI read-outs of hepatocytes inoculated with serial sporozoite dilutions of the 'All_Nluc' line in 384-well plates. Sporozoites were added to primary rhesus hepatocyte cultures in 384-well plates and cultured for 6 days until harvest. Quadruplicate wells were harvested for bioluminescence (expressed as relative light units (RLU)) or were fixed for HCI to assess the EEF numbers. Fluc signals versus total EEF counts (left panel) and Nluc signals versus total EEF counts (right panel) are depicted. Results are expressed as mean ± s.d. from one experiment representative of three experiments.

sporozoite dose (resulting in low EEF numbers), Nluc bioluminescence was clearly detected. The Fluc RLU value at this dose (23 ± 9) was low and only marginally above background (14 ± 5).

To assess whether we could sensitively detect hypnozoites in 384-well plates, we treated cultures from day 0−6 with atovaquone to eliminate the schizonts. Measurement of the (schizont-specific) Fluc signals of the atovaquone treated wells of the 'All_Nluc' line showed that luciferase signals had dropped to background levels as measured in uninfected hepatocytes, indicating schizont killing (Figure 7, left panel).

The Nluc signals (measuring both schizonts and hypnozoites) of atovaquone-treated cultures were about 30 times lower than the untreated control, due to the absence of schizonts. However, a robust signal, around 25 times higher than that of uninfected hepatocytes was still measured, representing the hypnozoites present in the culture (Figure 7, middle panel). Given that the Fluc signals are inherently lower than the Nluc signals,[23] the reference line 'Sz_Nluc' (expressing Nluc under control of *lisp2* regions) was subjected side by side to atovaquone treatment. As expected, in this line Nluc levels returned to background following atovaquone treatment, indicating that atovaquone treatment indeed had resulted in complete killing of schizonts (Figure 7, right panel). This demonstrates that also in a 384-well plate format, hypnozoites can be robustly measured by bioluminescence.

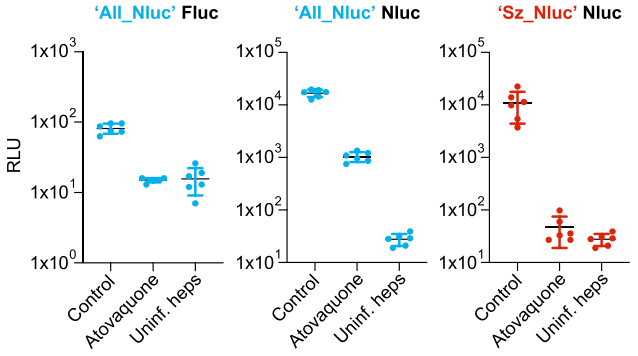

Figure 7. Bioluminescence signals expressed as relative light units (RLU) of the 'All_Nluc' line (blue) and the 'Sz_Nluc' line (red) with or without 1 μM atovaquone (d0−6) treatment. For each condition, measurements of 6 wells of a 384-well plate are depicted, including mean ± s.d..

CONCLUSION

The much-needed search for new compounds with anti-hypnozoite activity requires robust and fast high-throughput screening platforms. This type of high-throughput platforms typically requires a bioluminescent read-out, but current antihypnozoite drug screening methods rely on a lengthy and complicated image-based read-out. We here report a new analytical method that is superior over the currently available procedures for hypnozoite detection in terms of speed and robustness. The method we developed uses a dual bioluminescence-based read-out resulting in a fundamentally different way of analysis which relies on enzymatic activity rather than parasite counts based on HCI.[16] Further optimization of this system is now warranted to develop it into a sensitive medium- to high-throughput drug assay to identify the much needed novel hypnozoiticidal compounds.

ASSOCIATED CONTENT

Supporting Information

The Supporting Information is available free of charge at https://pubs.acs.org/doi/10.1021/acs.analchem.0c00547.

IC50 values (Table S1), cloning scheme (Figure S1), PI4K inhibitor activity (Table S2), and HCI images of drug treated wells and controls (Figure S2) (PDF)

AUTHOR INFORMATION

Corresponding Author

Clemens H. M. Kocken − *Department of Parasitology, Biomedical Primate Research Centre, 2288 GJ Rijswijk, The Netherlands*; Email: kocken@bprc.nl

Authors

Annemarie M. Voorberg-van der Wel − *Department of Parasitology, Biomedical Primate Research Centre, 2288 GJ Rijswijk, The Netherlands*; orcid.org/0000-0001-9403-0515

Anne-Marie Zeeman − *Department of Parasitology, Biomedical Primate Research Centre, 2288 GJ Rijswijk, The Netherlands*

Ivonne G. Nieuwenhuis − *Department of Parasitology, Biomedical Primate Research Centre, 2288 GJ Rijswijk, The Netherlands*

Nicole M. van der Werff − *Department of Parasitology, Biomedical Primate Research Centre, 2288 GJ Rijswijk, The Netherlands*

https://dx.doi.org/10.1021/acs.analchem.0c00547
Anal. Chem. 2020, 92, 6667−6675

Els J. Klooster − *Department of Parasitology, Biomedical Primate Research Centre, 2288 GJ Rijswijk, The Netherlands*
Onny Klop − *Department of Parasitology, Biomedical Primate Research Centre, 2288 GJ Rijswijk, The Netherlands*
Lars C. Vermaat − *Department of Parasitology, Biomedical Primate Research Centre, 2288 GJ Rijswijk, The Netherlands*

Complete contact information is available at: https://pubs.acs.org/10.1021/acs.analchem.0c00547

Author Contributions

The manuscript was written through contributions of all authors. All authors have given approval to the final version of the manuscript.

Notes

The authors declare no competing financial interest.

■ ACKNOWLEDGMENTS

We are grateful to Novartis (NITD) for supplying the PI4K compound and KAF156 and MMV for supplying atovaquone. We thank Brice Campo for continued support and the members of the Animal Science Department for excellent animal care and veterinary assistance. We acknowledge Francisca van Hassel for preparing graphical representations and the mosquito breeding facilities in Nijmegen for provision of *Anopheles stephensi* mosquitoes. This work was funded by the Bill & Melinda Gates Foundation (OPP1141292).

■ REFERENCES

(1) WHO. World malaria report, 2018.
(2) Price, R. N.; Tjitra, E.; Guerra, C. A.; Yeung, S.; White, N. J.; Anstey, N. M. *Am. J. Trop. Med. Hyg.* **2007**, *77* (6 Suppl), 79−87.
(3) Galinski, M. R.; Barnwell, J. W. *Malar. J.* **2008**, *7 Suppl 1*, S9.
(4) WHO. Global Technical Strategy for Malaria 2016−2030.
(5) Krotoski, W. A.; Krotoski, D. M.; Garnham, P. C.; Bray, R. S.; Killick-Kendrick, R.; Draper, C. C.; Targett, G. A.; Guy, M. W. *Br Med. J.* **1980**, *280* (6208), 153−4.
(6) Krotoski, W. A.; Garnham, P. C.; Bray, R. S.; Krotoski, D. M.; Killick-Kendrick, R.; Draper, C. C.; Targett, G. A.; Guy, M. W. *Am. J. Trop. Med. Hyg.* **1982**, *31* (1), 24−35.
(7) Campo, B.; Vandal, O.; Wesche, D. L.; Burrows, J. N. *Pathog. Global Health* **2015**, *109* (3), 107−22.
(8) Lacerda, M. V. G.; Llanos-Cuentas, A.; Krudsood, S.; Lon, C.; Saunders, D. L.; Mohammed, R.; Yilma, D.; Batista Pereira, D.; Espino, F. E. J.; Mia, R. Z.; Chuquiyauri, R.; Val, F.; Casapia, M.; Monteiro, W. M.; Brito, M. A. M.; Costa, M. R. F.; Buathong, N.; Noedl, H.; Diro, E.; Getie, S.; Wubie, K. M.; Abdissa, A.; Zeynudin, A.; Abebe, C.; Tada, M. S.; Brand, F.; Beck, H. P.; Angus, B.; Duparc, S.; Kleim, J. P.; Kellam, L. M.; Rousell, V. M.; Jones, S. W.; Hardaker, E.; Mohamed, K.; Clover, D. D.; Fletcher, K.; Breton, J. J.; Ugwuegbulam, C. O.; Green, J. A.; Koh, G. *N. Engl. J. Med.* **2019**, *380* (3), 215−228.
(9) Baird, J. K.; Battle, K. E.; Howes, R. E. *Malar. J.* **2018**, *17* (1), 42.
(10) Dembele, L.; Gego, A.; Zeeman, A. M.; Franetich, J. F.; Silvie, O.; Rametti, A.; Le Grand, R.; Dereuddre-Bosquet, N.; Sauerwein, R.; van Gemert, G. J.; Vaillant, J. C.; Thomas, A. W.; Snounou, G.; Kocken, C. H.; Mazier, D. *PLoS One* **2011**, *6* (3), No. e18162.
(11) Zeeman, A. M.; van Amsterdam, S. M.; McNamara, C. W.; Voorberg-Van der Wel, A.; Klooster, E. J.; van den Berg, A.; Remarque, E. J.; Plouffe, D. M.; van Gemert, G. J.; Luty, A.; Sauerwein, R.; Gagaring, K.; Borboa, R.; Chen, Z.; Kuhen, K.; Glynne, R. J.; Chatterjee, A. K.; Nagle, A.; Roland, J.; Winzeler, E. A.; Leroy, D.; Campo, B.; Diagana, T. T.; Yeung, B. K.; Thomas, A. W.; Kocken, C. H. *Antimicrob. Agents Chemother.* **2014**, *58* (3), 1586−95.
(12) Gural, N.; Mancio-Silva, L.; Miller, A. B.; Galstian, A.; Butty, V. L.; Levine, S. S.; Patrapuvich, R.; Desai, S. P.; Mikolajczak, S. A.; Kappe, S. H. I.; Fleming, H. E.; March, S.; Sattabongkot, J.; Bhatia, S. N. *Cell Host Microbe* **2018**, *23* (3), 395−406 e4..
(13) Roth, A.; Maher, S. P.; Conway, A. J.; Ubalee, R.; Chaumeau, V.; Andolina, C.; Kaba, S. A.; Vantaux, A.; Bakowski, M. A.; Thomson-Luque, R.; Adapa, S. R.; Singh, N.; Barnes, S. J.; Cooper, C. A.; Rouillier, M.; McNamara, C. W.; Mikolajczak, S. A.; Sather, N.; Witkowski, B.; Campo, B.; Kappe, S. H. I.; Lanar, D. E.; Nosten, F.; Davidson, S.; Jiang, R. H. Y.; Kyle, D. E.; Adams, J. H. *Nat. Commun.* **2018**, *9* (1), 1837.
(14) Fan, F.; Wood, K. V. *Assay Drug Dev. Technol.* **2007**, *5* (1), 127−36.
(15) Derbyshire, E. R.; Prudencio, M.; Mota, M. M.; Clardy, J. *Proc. Natl. Acad. Sci. U. S. A.* **2012**, *109* (22), 8511−6.
(16) Swann, J.; Corey, V.; Scherer, C. A.; Kato, N.; Comer, E.; Maetani, M.; Antonova-Koch, Y.; Reimer, C.; Gagaring, K.; Ibanez, M.; Plouffe, D.; Zeeman, A. M.; Kocken, C. H.; McNamara, C. W.; Schreiber, S. L.; Campo, B.; Winzeler, E. A.; Meister, S. *ACS Infect. Dis.* **2016**, *2* (4), 281−293.
(17) Deye, G. A.; Gettayacamin, M.; Hansukjariya, P.; Im-Erbsin, R.; Sattabongkot, J.; Rothstein, Y.; Macareo, L.; Fracisco, S.; Bennett, K.; Magill, A. J.; Ohrt, C. *Am. J. Trop. Med. Hyg.* **2012**, *86* (6), 931−5.
(18) Kocken, C. H.; van der Wel, A.; Thomas, A. W. *Exp. Parasitol.* **1999**, *93* (1), 58−60.
(19) Akinyi, S.; Hanssen, E.; Meyer, E. V.; Jiang, J.; Korir, C. C.; Singh, B.; Lapp, S.; Barnwell, J. W.; Tilley, L.; Galinski, M. R. *Mol. Microbiol.* **2012**, *84* (5), 816−31.
(20) Voorberg-Van der Wel, A.; Zeeman, A. M.; van Amsterdam, S. M.; van den Berg, A.; Klooster, E. J.; Iwanaga, S.; Janse, C. J.; van Gemert, G. J.; Sauerwein, R.; Beenhakker, N.; Koopman, G.; Thomas, A. W.; Kocken, C. H. *PLoS One* **2013**, *8* (1), No. e54888.
(21) Voorberg-Van der Wel, A.; Roma, G.; Gupta, D. K.; Schuierer, S.; Nigsch, F.; Carbone, W.; Zeeman, A. M.; Lee, B. H.; Hofman, S. O.; Faber, B. W.; Knehr, J.; Pasini, E.; Kinzel, B.; Bifani, P.; Bonamy, G. M. C.; Bouwmeester, T.; Kocken, C. H. M.; Diagana, T. T., A comparative transcriptomic analysis of replicating and dormant liver stages of the relapsing malaria parasite Plasmodium cynomolgi. *Elife* 2017, *6*.
(22) Bertschi, N. L.; Voorberg-Van der Wel, A.; Zeeman, A. M.; Schuierer, S.; Nigsch, F.; Carbone, W.; Knehr, J.; Gupta, D. K.; Hofman, S. O.; van der Werff, N.; Nieuwenhuis, I.; Klooster, E.; Faber, B. W.; Flannery, E. L.; Mikolajczak, S. A.; Chuenchob, V.; Shrestha, B.; Beibel, M.; Bouwmeester, T.; Kangwanrangsan, N.; Sattabongkot, J.; Diagana, T. T.; Kocken, C. H.; Roma, G., Transcriptomic analysis reveals reduced transcriptional activity in the malaria parasite Plasmodium cynomolgi during progression into dormancy. *Elife* 2018, *7*.
(23) Hall, M. P.; Unch, J.; Binkowski, B. F.; Valley, M. P.; Butler, B. L.; Wood, M. G.; Otto, P.; Zimmerman, K.; Vidugiris, G.; Machleidt, T.; Robers, M. B.; Benink, H. A.; Eggers, C. T.; Slater, M. R.; Meisenheimer, P. L.; Klaubert, D. H.; Fan, F.; Encell, L. P.; Wood, K. V. *ACS Chem. Biol.* **2012**, *7* (11), 1848−57.
(24) England, C. G.; Ehlerding, E. B.; Cai, W. *Bioconjugate Chem.* **2016**, *27* (5), 1175−1187.
(25) Gupta, D. K.; Dembele, L.; Voorberg-Van der Wel, A.; Roma, G.; Yip, A.; Chuenchob, V.; Kangwanrangsan, N.; Ishino, T.; Vaughan, A. M.; Kappe, S. H.; Flannery, E. L.; Sattabongkot, J.; Mikolajczak, S.; Bifani, P.; Kocken, C. H.; Diagana, T. T., The Plasmodium liver-specific protein 2 (LISP2) is an early marker of liver stage development. *Elife* 2019, *8*.
(26) Voorberg-Van der Wel, A. M.; Zeeman, A. M.; Nieuwenhuis, I. G.; van der Werff, N. M.; Klooster, E. J.; Klop, O.; Vermaat, L. C.; Gupta, D. K.; Dembele, L.; Diagana, T. T.; Kocken, C. H. M. *Communications Biology* **2020**, *3* (1), 7.
(27) Pasini, E. M.; Bohme, U.; Rutledge, G. G.; Voorberg-Van der Wel, A.; Sanders, M.; Berriman, M.; Kocken, C. H.; Otto, T. D. *Wellcome Open Res.* **2017**, *2*, 42.
(28) Feldmann, A. M.; Ponnudurai, T. *Med. Vet Entomol* **1989**, *3* (1), 41−52.

(29) Guguen-Guillouzo, C.; Campion, J. P.; Brissot, P.; Glaise, D.; Launois, B.; Bourel, M.; Guillouzo, A. *Cell Biol. Int. Rep.* **1982**, *6* (6), 625−8.
(30) Zou, B.; Nagle, A.; Chatterjee, A. K.; Leong, S. Y.; Tan, L. J.; Sim, W. L.; Mishra, P.; Guntapalli, P.; Tully, D. C.; Lakshminarayana, S. B.; Lim, C. S.; Tan, Y. C.; Abas, S. N.; Bodenreider, C.; Kuhen, K. L.; Gagaring, K.; Borboa, R.; Chang, J.; Li, C.; Hollenbeck, T.; Tuntland, T.; Zeeman, A. M.; Kocken, C. H.; McNamara, C.; Kato, N.; Winzeler, E. A.; Yeung, B. K.; Diagana, T. T.; Smith, P. W.; Roland, J. *ACS Med. Chem. Lett.* **2014**, *5* (8), 947−50.
(31) De Niz, M.; Stanway, R. R.; Wacker, R.; Keller, D.; Heussler, V. T. *Malar. J.* **2016**, *15*, 232.
(32) Azevedo, M. F.; Nie, C. Q.; Elsworth, B.; Charnaud, S. C.; Sanders, P. R.; Crabb, B. S.; Gilson, P. R. *PLoS One* **2014**, *9* (11), No. e112571.
(33) Straimer, J.; Lee, M. C.; Lee, A. H.; Zeitler, B.; Williams, A. E.; Pearl, J. R.; Zhang, L.; Rebar, E. J.; Gregory, P. D.; Llinas, M.; Urnov, F. D.; Fidock, D. A. *Nat. Methods* **2012**, *9* (10), 993−8.
(34) Zeeman, A. M.; Lakshminarayana, S. B.; van der Werff, N.; Klooster, E. J.; Voorberg-Van der Wel, A.; Kondreddi, R. R.; Bodenreider, C.; Simon, O.; Sauerwein, R.; Yeung, B. K.; Diagana, T. T.; Kocken, C. H. *Antimicrob. Agents Chemother.* **2016**, *60* (5), 2858−63.
(35) Paquet, T.; Le Manach, C.; Cabrera, D. G.; Younis, Y.; Henrich, P. P.; Abraham, T. S.; Lee, M. C. S.; Basak, R.; Ghidelli-Disse, S.; Lafuente-Monasterio, M. J.; Bantscheff, M.; Ruecker, A.; Blagborough, A. M.; Zakutansky, S. E.; Zeeman, A. M.; White, K. L.; Shackleford, D. M.; Mannila, J.; Morizzi, J.; Scheurer, C.; Angulo-Barturen, I.; Martinez, M. S.; Ferrer, S.; Sanz, L. M.; Gamo, F. J.; Reader, J.; Botha, M.; Dechering, K. J.; Sauerwein, R. W.; Tungtaeng, A.; Vanachayangkul, P.; Lim, C. S.; Burrows, J.; Witty, M. J.; Marsh, K. C.; Bodenreider, C.; Rochford, R.; Solapure, S. M.; Jimenez-Diaz, M. B.; Wittlin, S.; Charman, S. A.; Donini, C.; Campo, B.; Birkholtz, L. M.; Hanson, K. K.; Drewes, G.; Kocken, C. H. M.; Delves, M. J.; Leroy, D.; Fidock, D. A.; Waterson, D.; Street, L. J.; Chibale, K., Antimalarial efficacy of MMV390048, an inhibitor of Plasmodium phosphatidylinositol 4-kinase. *Sci. Transl Med.* 2017, *9* (387).

https://dx.doi.org/10.1021/acs.analchem.0c00547
Anal. Chem. 2020, 92, 6667−6675